Leakage pathway estimation using iTOUGH2 in a multiphase flow system for geologic CO_2 storage

Seong Jun Lee, Brian J. McPherson & Fernando Guevara Vasquez

Environmental Earth Sciences

ISSN 1866-6280

Environ Earth Sci
DOI 10.1007/s12665-015-4523-3

Springer

Environ Earth Sci
DOI 10.1007/s12665-015-4523-3

ORIGINAL ARTICLE

Leakage pathway estimation using iTOUGH2 in a multiphase flow system for geologic CO_2 storage

Seong Jun Lee[1] · **Brian J. McPherson**[1] · **Fernando Guevara Vasquez**[2]

Received: 3 December 2014 / Accepted: 11 May 2015

Abstract The objective of this study is to apply an inverse analysis using the iTOUGH2 model to estimate the location of a leakage pathway in multiple brine reservoirs when CO_2 is injected. If a reservoir exhibits leakage, brine or CO_2 is able to migrate into a permeable reservoir overlying the storage reservoir. Fluid pressure anomalies induced by leaks in the overlying reservoir can be distributed differently depending on the leakage locations and rates. Thus, the application of an inverse model utilizes specific pressure anomalies for leakage pathway detection. Prior to applying the inverse analysis, a forward simulation and a sensitivity analysis are conducted. The result of forward simulation demonstrates the interrelation between migrations of brine or CO_2 through the leakage pathway and pressure anomalies in the leakage pathway and reservoirs. The sensitivity analysis is performed to evaluate/identify the most influential model inputs on the observed pressure signals and the most appropriate monitoring wells for leakage pathway estimation. The inverse modeling examines the impact of the input parameter's uncertainties, the number of monitoring wells, observed periods of leakage signal, and noises in the measurements on the leakage pathway estimation through thirteen simulation scenarios. Residual (between the measured pressure and the calculated pressure) analysis illustrates that pressure anomalies in the overlying reservoir induced by leaks are critical information for leakage pathway estimation. The accuracy of the leakage detection using inverse analysis can significantly depend on the number of monitoring wells and the magnitude of the pressure anomalies.

Keywords Inverse analysis · Leakage pathway detection · Geologic carbon storage · Pressure anomalies in overlying formation · Pressure monitoring

Introduction

The objective of this study is to apply mathematical inverse analysis to identify possible locations of abandoned wells or other possible leakage zones, in subsurface reservoirs. This research is related to the storage of CO_2, a primary greenhouse gas from coal fired power plants and other point sources, in geological formations. This research focuses on the storage of CO_2 in saline aquifers. However, the storage of CO_2 in deep geological formations has risks, and perhaps the most important risk is the leakage of CO_2 (Metz et al. 2005). For a reservoir to store CO_2, it will ideally exhibit high porosity and high permeability and be capped by a low-permeability seal layer (or caprock above the reservoir). The existence of pathways that can release CO_2 from the reservoir and through the seal rock layer may allow CO_2 to escape into the atmosphere or to migrate into adjacent reservoirs. CO_2 leakage through abandoned pre-existing wells is identified as one of the most probable leakage pathways. More than 350,000 abandoned oil and gas wells have been drilled in Alberta, Canada (Gasda et al. 2004). Particularly, uncompleted or improperly plugged abandoned wells are the most susceptible to the leakage of buoyant fluids such as CO_2 (Metz et al. 2005). In geologic carbon storage (GCS), the detection of these pathways is a very significant objective.

✉ Seong Jun Lee
sjlee@egi.utah.edu

[1] Department of Civil and Environmental Engineering, University of Utah, Salt Lake City, UT 84112, USA

[2] Department of Mathematics, University of Utah, Salt Lake City, UT 84112, USA

Published online: 20 May 2015

In GCS, many researchers have studied forward modeling to solve leakage problems. For example, Pruess and García (2002) modeled the effects of CO_2 discharge along a fault zone, including the impacts of salinity on CO_2 migration. In addition, Pruess and García (2002) considered how decreasing pressure reduces fluid mobility, thus decreasing vertical CO_2 flow but increasing the lateral migration of CO_2. Doughty and Pruess (2004) investigated the effects of heterogeneity on CO_2 migration. Altevogt and Celia (2004) explored flux mechanisms (of CO_2 transport) in the vadose zone. Nordbotten et al. (2004) studied perturbations in hydraulic heads that were induced by leakage rates through abandoned wells in systems with two aquifers and one aquitard. Nordbotten et al. (2008) studied CO_2 leakage in multiple geological layers. Zhou et al. (2009) developed semi-analytical solutions to simulate induced pressure perturbations and vertical leakage rates in a system consisting of multiple aquifers. Cihan et al. (2011) studied a methodology to solve pressure perturbations through leakage wells and associated groundwater injection/pumping. Nogues et al. (2011) investigated the limits and extents of monitoring wells to measure pressure anomalies induced by leakage wells. Hou et al. (2012) quantified the post-injection impacts of CO_2 leakage through heterogeneous caprock without specific leakage pathways.

However, fewer people are interested in the application of inverse modeling for leakage estimation than those using forward modeling to evaluate leakage features. Gasda et al. (2011) investigated the actual permeability of several wells in the field using what is called the "Vertical Interference Test" (VIT) to measure pressure related to fluid movement outside of well casings. Jung et al. (2012a) developed a framework for early leakage detection. The framework consists of inverse modeling with high-spatial-resolution surface deformation (InSAR) data. Jung et al. (2012b) also utilized inverse modeling for leakage detection in a single-phase system. Pressure anomalies from monitoring wells in multiple reservoirs were used for early leakage detection by inverse modeling. They introduced monitoring data with random errors resulting from various sources and systematic errors due to drift in pressure gauges and uncertain values for caprock permeability. Jung et al. (2013) examined the sensitivity of pressure anomalies by leakage. They suggested that accurate information regarding the formation parameters (like formation permeability) is indeed more important than leaky well permeability for the successful detection of leaky wells. In addition, they concluded that the level of noise in the measured signals is also significant for leakage pathway detection. However, they focused on the simple single-phase problem. Other methods for the risk assessment of CO_2 leaks include InSAR data of surface deformation, water chemistry perturbations in aquifers and CO_2 land surface flux monitoring (Carroll et al. 2009; Krevor et al. 2010; Onuma and Ohkawa 2009).

Abandoned wells and other leakage pathways typically exhibit higher vertical permeability than the confining layers and reservoirs. The leakage pathways may cause pressure anomalies that induce transient flow in reservoirs. Thus, this study focuses in particular on pressure anomalies to estimate the locations of abandoned wells and other potential leakage zones. Before applying inverse methods to identify leakage pathways, more general numerical modeling is performed to evaluate the impacts of leakage zones on the flow patterns in confined brine aquifers with homogeneous and isothermal conditions. The uncertainties of the model parameters are of major consideration for the successful estimation of leakage pathways (because the model parameters with errors are assigned as known values in the inverse modeling). Sensitivity analysis is implemented to examine the effects of the uncertainties in geological properties on the magnitude of the pressure and to evaluate the sensitivities of the pressure at the monitoring wells to the leakage pathway permeability. To achieve these objectives, this study uses iTOUGH2, a simulation code developed by the Lawrence Berkeley National Laboratory (Finsterle 2007).

Materials and methods

Conceptual framework of inverse modeling

If a reservoir exhibits leakage, a leakage pathway can induce pressure anomalies in adjacent reservoirs overlying the storage reservoir, i.e., brine or CO_2 is able to move into the overlying permeable reservoir from the source reservoir. Fluid pressure perturbations can be distributed and propagated differently throughout the source and overlying reservoirs depending on the leakage locations and rates. However, specific pressure anomalies induced from leakage can provide information about the leakage locations and rates. The inverse method employed here estimates the leakage locations and rates by calculating the discrepancy between the calculated and observed pressure data at monitoring wells. The objective function (S) is used to calculate the discrepancy at points in identical space and time, referred to as calibration points. The weighted least-squares objective function used by iTOUGH2 is

$$S = \sum_{i=1}^{m} \frac{r_i^2}{\sigma_{z_i}^2}. \quad (1)$$

Here, i is calibration point ($i = 1,\ldots, m$), r_i is residuals between the measured pressure (z_i^*) and calculated pressure (z_i), i.e., $r_i = z_i^* - z_i$, and $\sigma_{z_i}^2$ is the prior error variance (or weighting coefficient) for each observation. The

measurement data can be appropriately weighted to be scaled and assessed based on the measurement and random errors (this problem is discussed in "Residual analysis" and "Effect of singular noises in the measurements" sections).

The calculated pressures are obtained through forward simulation [TOUGH2 coupled with the ECO2N module, an equation of state module for mixtures of water, NaCl, and CO_2 (Pruess et al. 1999)] parameterized with the vertical permeability values of randomly selected "initial guess locations" of leakage pathways, which will be updated as part of the optimization approach. The forward simulation is repeated with updated parameter values, and when the discrepancies are minimized, the resulting parameter values are deemed the best estimates. An initial guess location with minimum objective function is estimated to the most likely leakage pathway location. The Levenberg–Marquardt algorithm designed for the minimization of a nonlinear least-squares models is applied to minimize the objective function in this study. Table 1 presents the inverse modeling procedure for leakage pathway estimation.

Model and parameters

A model domain is designed and parameterized for the simulation of CO_2 storage and leakage. For an idealized system to realize pressure perturbations induced by CO_2 injection and leakage, the model domain should ideally consist of at least three layers, such as two sandstone layers and one confining layer for this analysis (Cihan et al. 2011). Figure 1 is a schematic of multiple formations with a single leakage pathway. The domain consists of a storage formation (for CO_2 injection through an injection well), a confining formation (caprock), and an overlying formation. The overlying and the storage formations are composed of sandstone with appropriate permeability, and the caprock consists of shale with lower permeability and is located in

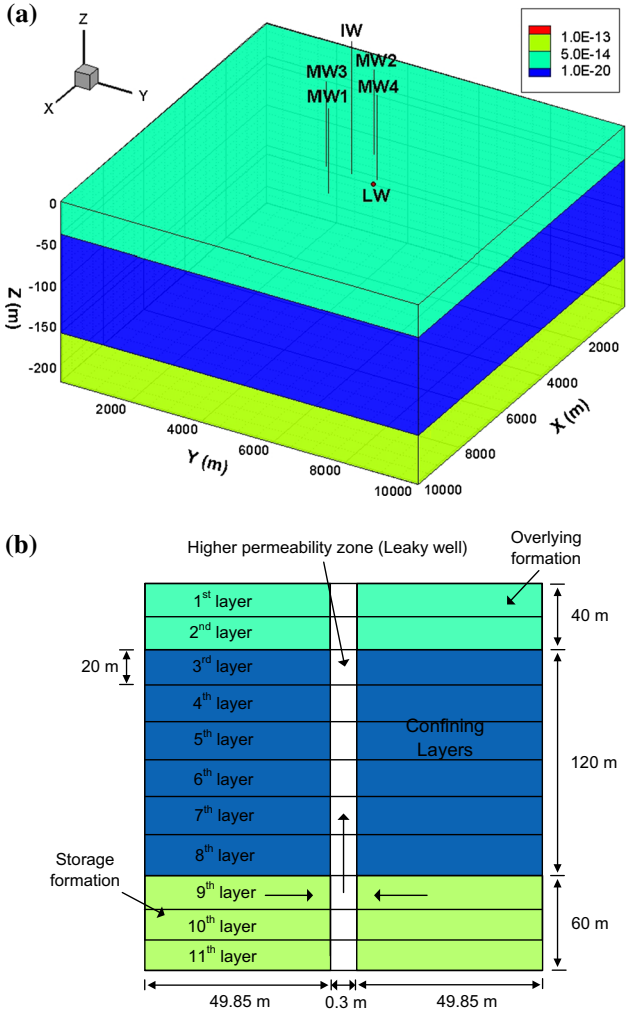

Fig. 1 Conceptual domain: **a** schematic of the model of multiple formations with a leakage pathway. The permeabilities of the storage reservoir, the caprock and the overlying formation are 10^{-13} m^2, 10^{-20} m^2 and 10^{-15} m^2, respectively. *IW* injection well, *MW* monitoring well, and *LW* leakage well. **b** Schematic of the specified LW (not to scale)

Table 1 Procedures of inverse modeling for leakage pathway estimation

Step	Description
1	Development of a forward conceptual model
2	Selection of initial guesses of leakage pathway locations
3	Assignment of vertical permeability of an initial guess and permeability of the formations (as the most influential parameters on calculated model response)
4	Calculation of TOUGH2
5	Calculation of discrepancy between the calculated and measured pressure at calibration points by an objective function
6	Updating the parameter values until minimum objective function values can be obtained or reaching the iteration number specified by the users
7	Iterating from Steps 3 through 6
8	A placement of initial guess with a minimum objective function value is estimated to the likely leakage location

the middle of the conceptual domain. The hydrogeological properties for both formations and caprock are assigned based on information on the deep geological formations for CO_2 storage from Metz et al. (2005). It is assumed that the entire domain is homogenous, isothermal (50 °C), and completely saturated by brine. The domain size is 10,100 m × 10,100 m × 220 m. The number of cells is 103 × 103 × 11 (116,699 grid blocks total). The XZ-planes on the left and right boundaries (Fig. 1a) are assigned a constant head boundary condition, but the other boundaries are assigned no flow boundary conditions. The assumed leakage pathway vertically penetrates the caprock at $(x, y) = (5250, 6050$ m) from the origin. Table 2 summarizes the dimensions and the parameters of the model. The initial pressures of all the top grid blocks and all the bottom grid blocks are specified as approximately 10 and 12 MPa, respectively, and the other cells are assigned a linear distribution with the same pressure gradient in the vertical direction to maintain the hydrostatic conditions before CO_2 injection. In addition, injected CO_2 can sustain supercritical conditions in the simulation domain. The porosity of the overlying and storage formations and the leakage pathway is 0.2, and the porosity of the caprock is assigned as 0.02. The pore compressibility (Pa^{-1}) is assumed as 0 in the model domain so that the porosity remains constant. This simulation is assigned a constant injection rate (63.4 kg/s) at $(x, y, z) = (5050, 5050, -190$ m) from the origin throughout the simulation time (10 years). Table 3 details the point locations of the monitoring wells. In the model domain, four monitoring wells are available for pressure observation. The four monitoring wells measure pressure data in both the overlying and storage formations (eight points total).

The van Genuchten–Mualem model (Mualem 1976; van Genuchten 1980) and the Corey model (Corey 1954) were used for the relative permeability function. The van Genuchten model (van Genuchten 1980) was implemented for the capillary pressure function. For further information on the relative permeability and capillary pressure functions, refer to Pruess (2005). Table 4 details the parameter values for the relative permeability and capillary pressure functions.

Forward simulation

The forward simulations show the pressure perturbation and migration of CO_2 through the leakage pathway. The pressure data at the simulated monitoring wells are used as "observed data" for the inverse simulation afterward. The migration of CO_2 along a leakage pathway saturated by brine can be subject to buoyant and capillary effects and may impact multi-dimensional flow in the formations (Pruess 2005). The conceptual domain in Fig. 1 with the given hydrogeological properties is employed to model the effects of CO_2 and brine migration through a leakage pathway. Figure 2 presents, the discharge rates of CO_2 and brine at the top of the leakage pathway. Figure 3 illustrates, the simulated pressure perturbations at the top of the leakage pathway. As shown in Fig. 2, when CO_2 injection starts, pressure buildup propagates to the top of the leakage pathway, at which point it induces brine discharge. The outflow of brine continues for approximately 1.1×10^8 s (3.5 years), so the pressure anomalies increase in the leakage pathway (see Fig. 3). However, CO_2 reaches the leakage pathway at that time, so brine discharge is rapidly reduced (see Fig. 2) because the relative permeability of brine decreases (due to the drop in brine saturation), and increased capillary pressure (due to the surface tension which exists at the interface between two immiscible fluids) also quickly reduces the pressure of brine (see Fig. 3). The rapid drop in brine pressure continues until the CO_2 pressure exceeds the capillary pressure to break through brine (see Fig. 3). After CO_2 breaks through at approximately 1.12×10^8 s (3.55 years), the flow rates of

Table 2 Dimensions and parameters of the conceptual model

Domain size (m)	10,100 × 10,100 × 220	Permeability (m^2)	Storage formation	$k_x = k_y = k_z = 10^{-13}$
Each normal cell size (m)	100 × 100 × 20		Overlying formation	$k_x = k_y = k_z = 10^{-15}$
Cell sizes including a leakage pathway (m)	49.85 × 49.85 × 20, 0.3 × 0.3 × 20 and 49.85 × 49.85 × 20		Caprock	$k_x = k_y = k_z = 10^{-20}$
Number of cells	103 × 103 × 11 (116,699 total)		Leakage pathway	$k_{lx} = k_{ly} = 10^{-20}$ and $k_{lz} = 10^{-10}$
Leakage pathway location from origin	(5250, 6050 m)	Porosity	Both aquifers	0.2
Simulation time (s)	0–3.16e8 (≈10 years)		Caprock	0.02
Time step size (s)	10	Tolerance	1.0e−7	

Table 3 Eight location points of the four monitoring wells and distance from a leakage pathway

	1st well (MW1)	2nd well (MW2)	3rd well (MW3)	4th well (MW4)
x, *y*, and *z* directional distances from origin (m)				
MP at OF	6050, 5050, −30	4050, 5050, −30	5050, 4050, −30	5050, 6050, −30
MP at SF	6050, 5050, −170	4050, 5050, −170	5050, 4050, −170	5050, 6050, −170
x and *y* directional distance from leakage pathway (m)				
–	800, 1000	1200, 1000	200, 2000	200, 0

MP measurement point, *OF* overlying formation, *SF* storage formation

Table 4 Relative permeability and capillary pressure parameters

	Parameter values
Relative permeability	
Liquid: van Genuchten–Mualem function	
Irreducible water saturation (S_{lr})	0.20
Exponent (λ)	0.457
Gas: Corey function	
Irreducible gas saturation (S_{gr})	0.05
Capillary pressure	
van Genuchten function	
Irreducible water saturation (S_{lr})	0.20
Exponent (λ)	0.475
Strength coefficient (P_0)	19.61 kPa
Maximum capillary pressure (P_{max})	10^4 kPa

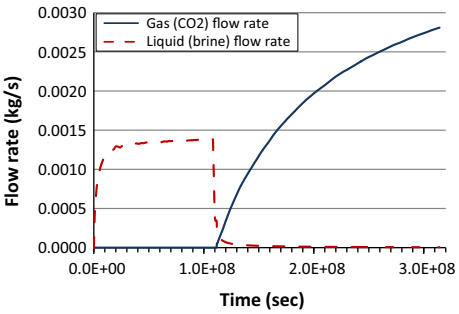

Fig. 2 Simulated CO_2/brine discharge rates at the *top* of the leakage pathway

CO_2 start to increase due to the higher relative permeability following increased CO_2 saturation (see Fig. 2). The CO_2 pressures, therefore, rapidly increase at the top of leakage pathway (see Fig. 3). In this paper, the pressure anomalies that occur when CO_2 breaks through the leakage pathway are referred to as "capillary effects." Figure 4 illustrates, the simulated pressure propagation induced by leaks in the XY-plane of the overlying formation. As mentioned earlier, when CO_2 reaches the leakage pathway, the brine leakage rates decrease in the leakage pathway due to capillary effects, so the pressures rapidly drop in the

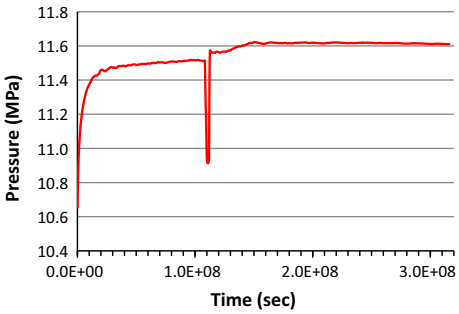

Fig. 3 Simulated pressure perturbations at the *top* of the leakage pathway

leakage pathway. The capillary effects also cause a decrease in the pressure propagation in the overlying formation (Fig. 4b, c). After the outflow of CO_2 breaks through the leakage pathway, the pressures continuously increase in the overlying formation until the end of the simulation (Fig. 4d). Figure 5 provides, the pressure profiles at the monitoring points in the overlying formation and in the storage formation. In Fig. 5a, each pressure profile for a monitoring well exhibits a sudden change in the pressure. One explanation is that the pressure anomalies caused by capillary effects at the leakage pathway propagate into the entire overlying reservoir. This propagation has a significant effect on MW4 in the overlying reservoir. Such information may be an indicator of CO_2 leakage through the leakage pathway. In Fig. 5b, the pressures increase after CO_2 reaches the monitoring wells due to capillary pressure at approximately 3.5 years.

Sensitivity analysis

A sensitivity analysis is conducted in terms of the pressure signals at the monitoring wells in the model domain (1) to quantify the impact of the uncertainties in input parameters on the calculated system response and (2) to identify more critical monitoring wells for leakage pathway estimation. First, the purpose of quantifying the uncertainties of the input parameters is to evaluate the most influential input parameters on the calculated pressures. The process will be a means to parameterize those input variables to reduce the

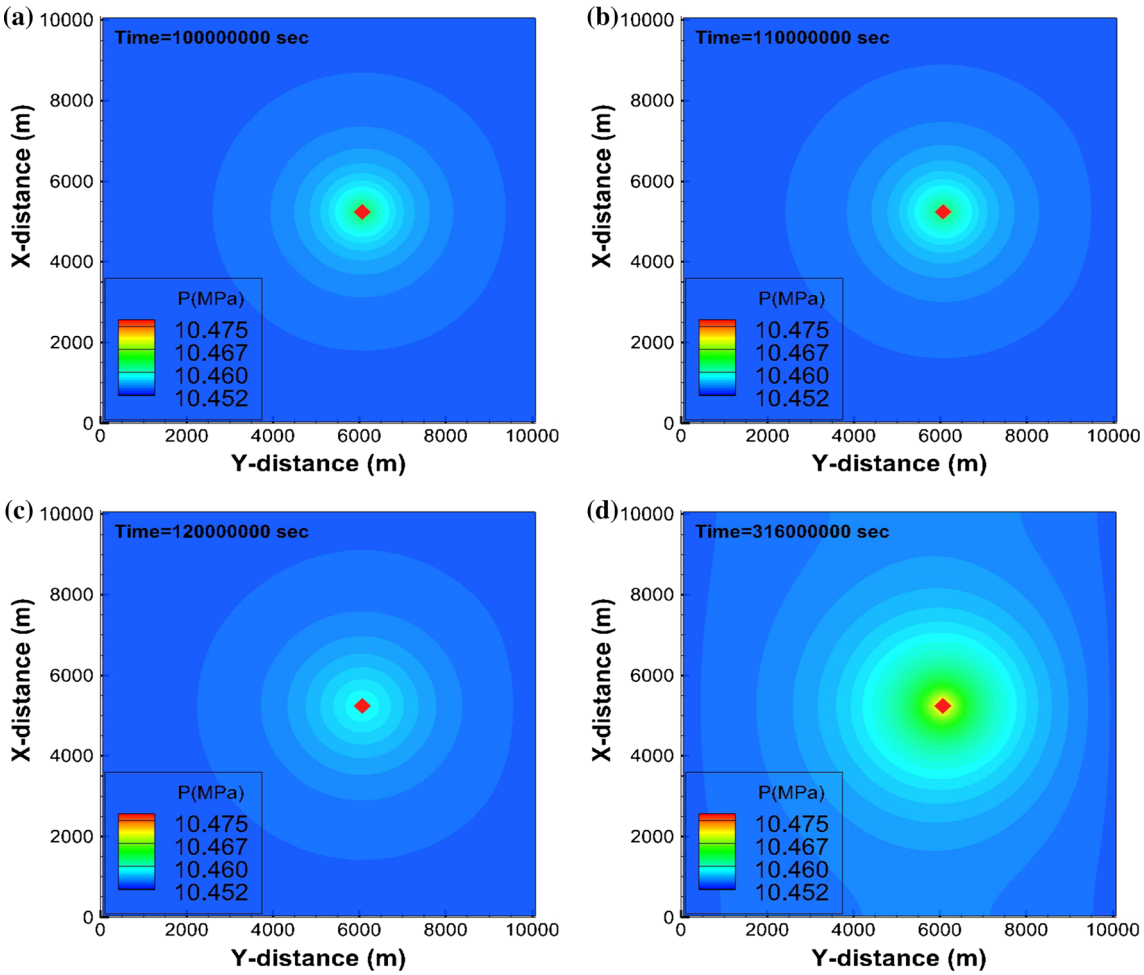

Fig. 4 Simulated pressure propagations in the XY-plane of the overlying formation **a** after 3.2 years, **b** after 3.5 years, **c** after 3.8 years, and **d** after 10 years

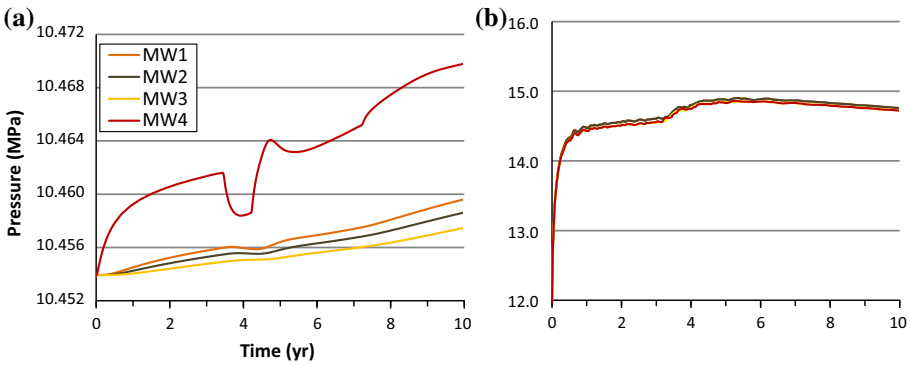

Fig. 5 Pressure profiles at the monitoring wells in **a** overlying and **b** storage formations

impact on a subsequent inversion. Second, for a successful inversion, the magnitude of the pressure anomalies induced by leakage can be important, and the changes in the permeability of leakage pathways, the main unknown parameter of this inverse analysis, should affect the pressures at the monitoring wells. The sensitivities of the pressures at the monitoring wells to changes in the leakage pathway permeability are examined to identify more critical monitoring wells.

This sensitivity analysis is conducted through the examination of a sigma-normalized coefficient ($\frac{\partial P}{\partial a} \cdot \frac{\sigma_a}{\sigma_P}$), where $\frac{\partial P}{\partial a}$ is sensitivity coefficient, P is pressure, a is parameter, and σ is standard deviation (Finsterle 2007; Saltelli et al.

2000). The sigma-normalized coefficient (SC) evaluates the difference in the calculated system response (pressure) to the change in each input parameter. A sensitivity analysis function of iTOUGH2 is utilized to examine the SC values for the given parameters. Jung et al. (2013) examined the sensitivity of pressure anomalies to the permeability of the overlying and storage aquifers, the leaky well permeability and the thicknesses of the overlying and storage aquifers. They suggested that the formation permeability has higher sensitivity and is more important for successful leaky well detection. Thus, in this study, the sensitivity analysis focuses on four input parameters: the vertical permeability of the leakage pathway (k_{lz}), permeability of the overlying formation k_O, permeability of the storage formation k_S, and caprock permeability (k_C). The initial parameter values of interest and their potential variations are assigned as shown in Table 5. The wide ranges of input factors are selected to evaluate the sensitivity to a simulated system response. In particular, the leakage pathway permeability values from 10^{-5} to 10^{-15} m^2 are assigned to represent a substantial leakage and less leakage cases (Cihan et al. 2013).

Figure 6 illustrates, the absolute SC values at eight location points of four monitoring wells (MW1, MW2, MW3, and MW4) from the sensitivity measures. In the overlying formation (Fig. 6a–d), the sensitivity of each k_O and k_S substantially increases depending on the decrease in the distance between the leakage pathway and the monitoring well (distance from the leakage pathway: MW3 > MW2 > MW1 > MW4). In total, both the k_O and k_S of the four input parameters are the most influential input parameters on the pressure signals at the MWs in the overlying formation. Note that the SC values of k_O and k_S rapidly increase and decrease after approximately 3.5 years. The rapid changes in the SC values are caused by capillary effects. The changes in k_O and k_S have a greater effect on the rapid pressure changes at the MWs near the leakage pathway. The sensitivity of k_C increases with time, especially after approximately 5 years, so k_C might also be considered an influential parameter if the observed leakage signals for over 5 years are used for the leakage pathway estimation. Pressure buildup in the storage formation (due to constant CO_2 injection) results in the migration (diffuse) of CO_2 or brine through the caprock (Cihan et al. 2013), so the changes in k_C affect the pressures in the overlying formation. In fact, the diffuse migration causes a decrease in the pressure anomalies in the overlying formation that were induced by leaks (Jung et al. 2012b). In addition, the thickness of the caprock has an effect on the diffuse migration. Refer to "Appendix 1" section for more details on the effects of caprock thickness on pressure anomalies induced by leaks. As shown in Fig. 6(e–h), k_S is the most influential parameter on the pressures at the MWs in the storage formation. The wide fluctuations of the SC values at all the MWs result from capillary pressures. These sensitivity analysis results indicate that prior information about the input parameters, particularly both k_O and k_S, is very important for the accuracy of pressure calculations. k_{lz} is much less sensitive than the other parameters at the MWs in both formations. The sensitivity analysis results of k_{lz} are depicted in Fig. 7 with an extended ordinate scale. As shown in Fig. 7, the SC values in the storage formation (Fig. 7b) are relatively very small for changes in the leakage rates (varied by k_{lz}), regardless of the increase in time. However, the SC values for the MWs in the overlying formation (Fig. 7a) are larger by approximately two orders of magnitude than those for the storage formation. In particular, at MW4, which is the closest MW to the leakage pathway, the difference in sensitivity between both formations is more significant. This result implies that the pressure signals in the overlying formation may be more important for leakage pathway detection through estimates of k_{lz}. The effects of the measurements in each formation on the leakage pathway estimation are discussed in "Residual analysis" section.

Inverse simulation

The calculated and measured system responses may include errors. In this context, error means a deviation between the calculated/measured and exact values. It is practically impossible to obtain exact values of calculated/measured system responses from the real world because the errors can never be removed. In general, both calculation (or modeling) error and measurement (or data) error have two types of errors: (1) systematic errors in the calculation

Table 5 Input parameter ranges for sensitivity analysis

Input parameters	Notation	Initial values	Variation	Minimum values	Maximum values
Leakage pathway permeability (m^2)	k_{lz}	1e−10	0.1	1e−15	1e−5
Overlying formation permeability (m^2)	k_O	1e−15	0.1	1e−16	1e−14
Storage formation permeability (m^2)	k_S	1e−13	0.1	1e−14	1e−12
Caprock permeability (m^2)	k_C	1e−20	0.1	1e−21	1e−19

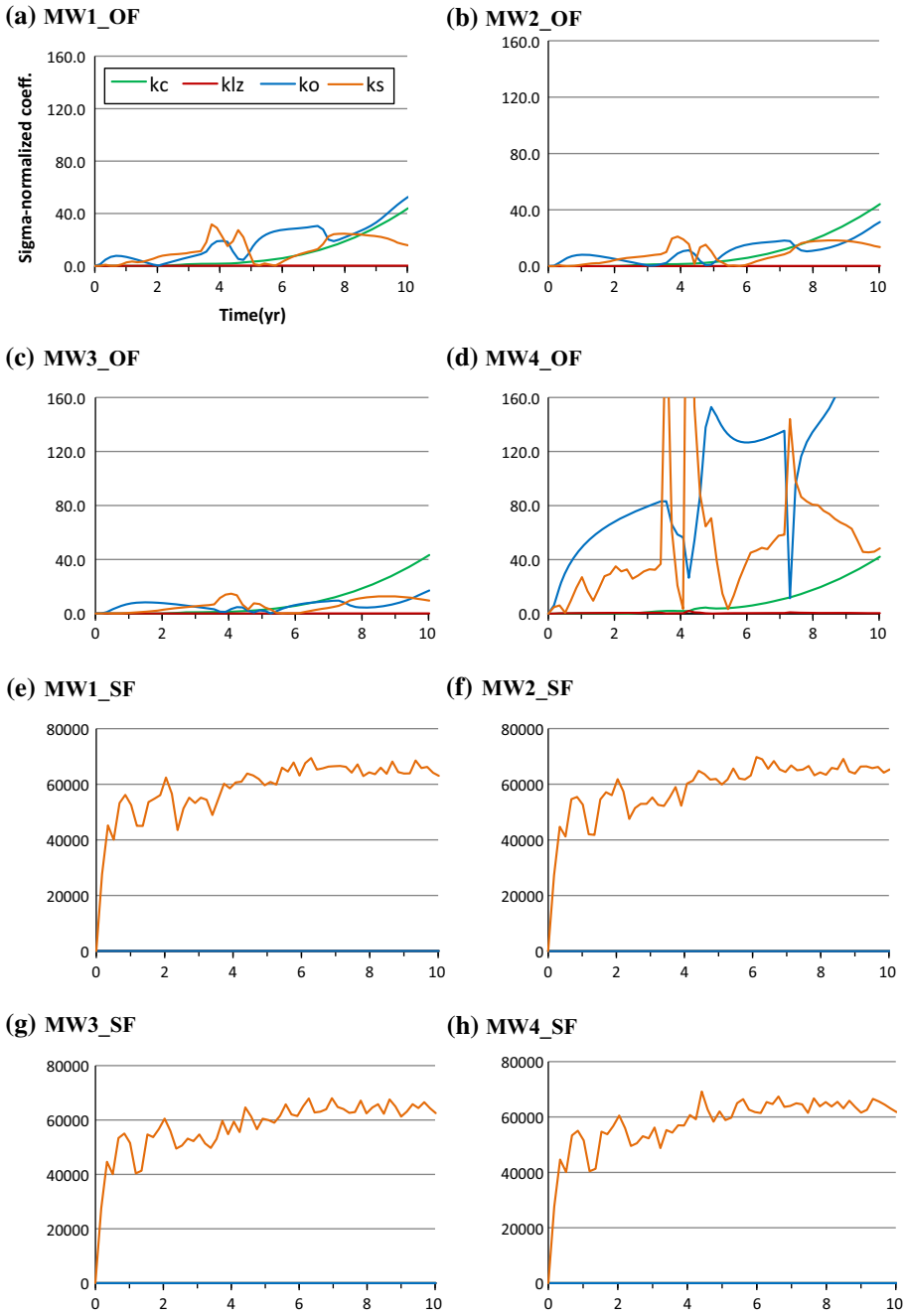

Fig. 6 Sensitivity analysis results for four input parameters at eight location points of four monitoring wells in both the overlying formation (OF) and storage formation (SF)

resulting from insufficient information about the input parameters and model geometry (systematic modeling error) and in the measurement due to drift in the pressure measuring devices (systematic data error), and (2) random errors in the modeling such as numerical oscillations (random modeling error) and in the measurement including noises (random data error). In most cases, the impact of systematic modeling errors is more significant than that of systematic data errors, while the random modeling errors are of less interest than the random data errors (Finsterle 2007). This study therefore focuses on examining the impact of both systematic modeling errors from uncertain input parameters and random data errors due to measured signals including random noises on inverse modeling.

Inverse modeling for the estimation of a leakage pathway is applied to the model domain of Fig. 1. However, the number of cells specified in the model domain ($103 \times 103 \times 11$) is adjusted to $21 \times 31 \times 11$ (7161 grid blocks total) to reduce the high computational demands for inverse modeling. The leakage pathway location is estimated by calibrating the logarithm of the absolute vertical permeability of each different initial guess location of the

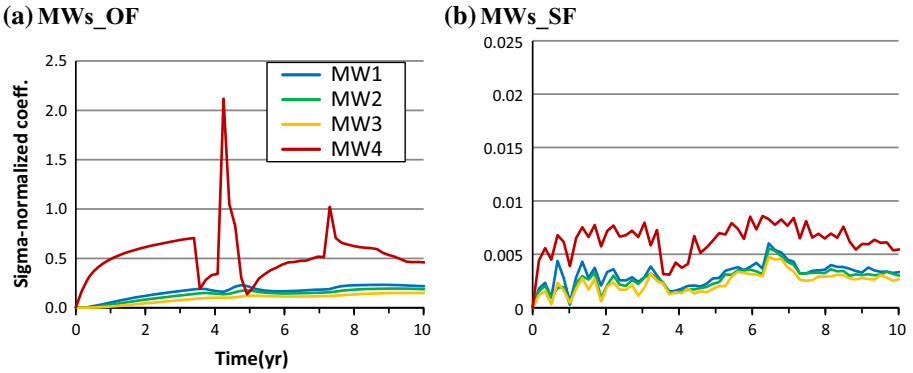

Fig. 7 Sensitivity analysis results for the permeability of the leakage pathway at eight location points in both the overlying formation (OF) and storage formation (SF)

leakage pathway. Forty-eight initial guess locations of the leakage pathway through the caprock at (z) = (−40 to −160 m) are randomly selected in a two-dimensional coordinate system (x, y) but are more densely assigned around an injection well located at the center of the model domain because significantly higher pressure in the region is likely to invoke potential CO_2 leakage. The grid blocks are meshed to 0.3 m × 0.3 m according to the specific geometry of each initial guess. Forty-eight inversions with each different initial guess location are performed to estimate a global minimum of the objective function, i.e., the most possible location of the leakage pathway.

Input parameter uncertainty is associated with the absolute permeability, porosity, relative permeability, and capillary pressure. Uncertainties are inherent to information regarding geologic and hydrologic boundaries and the thicknesses of geologic layers. However, it is impossible to examine or estimate all the uncertainties of those parameters through inverse modeling. In practice, a priori investigation of those parameters should be performed to reduce the associated error. Based on the results of the previous sensitivity analysis, the application focuses on evaluating and reducing the impact of uncertain permeability values from the reservoirs on the solutions of inverse modeling. In addition, the accuracy (or limit) of the inversions can be closely related to the number and network of monitoring wells and the observation periods at the monitoring wells of leakage signals that increase with CO_2 injection. To examine the effect of noises in the measurements on the parameter estimations, the observed signals randomly include an additive zero mean Gaussian noise that is ±0.1 % of the magnitude of each pressure data point at all the monitoring wells. Considering different combinations of those influential factors on the inverse modeling, the inverse modeling was applied to thirteen application examples. Cases 1, 2, and 3 examine the impact of reservoir permeability uncertainties, and case 4 identifies that the parameterization of the uncertain permeability values can reduce their impact using pure pressure signals (without data noise) from four monitoring wells when the entire monitoring period (10 years) is employed. Based on the result of case 4, cases 5–8 utilize the pure pressure signals from different combinations of two (MW2 and MW3) or three (MW1, MW2, and MW3) monitoring wells and monitoring periods of 1 or 3 years. The inverse modeling of cases 9 through 13 applies the pressure signals with data noises to cases 4 through 8. Table 6 summarizes the numbers and kinds of unknown parameters to be estimated, the observation periods, and the number and locations of the monitoring wells and data noise conditions in the measurements in each inverse modeling scenario.

Results

Inverse modeling results using pure pressure signals

Case 1 estimates only the location of the actual leakage pathway from the initial guesses based on the exact permeabilities of the overlying formation (10^{-15} m^2) and storage formation (10^{-13} m^2). This scenario can be called the "idealized case". The second case is inverse analysis for only the leakage location estimation based on an assumed error of the permeability field of the overlying formation (that permeability is $10^{-15.5}$ m^2). In case 3, the inverse modeling is also performed for only the calibration of the leakage location based on an assumed permeability error of the storage formation ($10^{-12.5}$ m^2). Case 4 simultaneously calibrates the uncertain formation permeabilities with the permeability of each potential leakage location through inverse modeling. Thus, the fourth inverse model estimates an optimal combination of three parameters: the logarithm of the vertical permeability of an initial guess location and the logarithms of the uncertain permeability values of both reservoirs. Figure 8 illustrates, each result from the eight cases using pure pressure signals with contour plots of the objective function values from forty-eight inversions with each different initial guess location. Figure 8a shows, the result of case 1 from four monitoring

Table 6 Numbers and kinds of unknown parameters to be estimated, data noise conditions, monitoring periods (time), and number of used monitoring wells (MWs) in thirteen inversion scenarios (perm. indicates permeability)

Case	# of MWs (MW name)	Data noise	Time (years)	# of unknown	Initial guess perm. (m^2)	Logarithm of applied OF perm. (m^2)			Logarithm of applied SF perm. (m^2)		
					Unknown	−15 (true)	−15.5	Unknown	−13 (true)	−12.5	Unknown
1	4 (1, 2, 3, 4)	N	10	1	Y	Y	–	N	Y	–	N
2	4 (1, 2, 3, 4)	N	10	1	Y	–	Y	N	Y	–	N
3	4 (1, 2, 3, 4)	N	10	1	Y	Y	–	N	–	Y	N
4	4 (1, 2, 3, 4)	N	10	3	Y	–	–	Y	–	–	Y
5	3 (1, 2, 3)	N	3	3	Y	–	–	Y	–	–	Y
6	2 (1, 2)	N	3	3	Y	–	–	Y	–	–	Y
7	3 (1, 2, 3)	N	1	3	Y	–	–	Y	–	–	Y
8	2 (1, 2)	N	1	3	Y	–	–	Y	–	–	Y
9	4 (1, 2, 3, 4)	Y	10	3	Y	–	–	Y	–	–	Y
10	3 (1, 2, 3)	Y	3	3	Y	–	–	Y	–	–	Y
11	2 (1, 2)	Y	3	3	Y	–	–	Y	–	–	Y
12	3 (1, 2, 3)	Y	1	3	Y	–	–	Y	–	–	Y
13	2 (1, 2)	Y	1	3	Y	–	–	Y	–	–	Y

wells. The inversion estimated the coordinate (x, y) = (5250, 6150 m) as the most possible location (black filled circle). The estimated leakage pathway has a deviation of 100 m against the actual leakage pathway location (void circle) at (x, y) = (5250, 6050 m). Even with the deviation of 100 m, the deviation is not significantly large with respect to the whole system, suggesting that the inversion results are qualitatively good. Case 2 resulted in a global minimum at (x, y) = (5150, 5750 m) for the predicted leakage pathway location as shown in Fig. 8b. The deviation from the actual leakage pathway location is approximately 316 m. Figure 8c illustrates that the leakage pathway location estimated for case 3 is (x, y) = (5150, 5950 m). The deviation between the actual and estimated leakage pathway is approximately 141 m. In cases 2 and 3, the two estimated leakage locations do not significantly deviate from the actual leakage pathway location. However, it can still be established that the uncertainty of the formation's permeability influences the accuracy of the inversion for the detection of the leakage pathway. The result from case 4 as shown in Fig. 8d has a deviation of 100 m from the actual leakage pathway location. The results indicate that estimating the combination of both the vertical permeability of each initial guess and the incorrect permeability values of the reservoirs reduces the impact of the uncertainty of the formation's permeability and increases the accuracy of the detection of the leakage pathway location. The specific accuracy of four inversion cases can be identified by the residual analysis in the next section.

Figure 8e–h illustrates each result of cases 5 through 8 estimated from three unknown parameters. In Fig. 8e, the contour plot has one global minimum (black filled circle) and two local minima (blue filled circles), but the deviation of the global minimum is 100 m from the actual leakage pathway location. Case 5, which had a combination of three monitoring wells and a three-year monitoring period, estimated an identical leakage pathway location as the idealized case. Meanwhile, the accuracies of cases 6, 7, and 8, which had certain combinations of fewer monitoring wells and monitoring periods, were reduced as shown in Fig. 8f–h. Case 8 of two well monitoring and 1-year monitoring scenario estimated two global minima (non-unique solution). Although the leakage pathway is well estimated in one of the two global minima, another estimated leakage pathway location has a significant deviation of 583 m from the actual leakage pathway. These inversion results indicate that the accuracy of inverse modeling can depend on the number of monitoring wells and the magnitude of the measured anomalous pressure induced by leaks at the monitoring wells. Refer to "Appendix 2" section for specific information regarding the magnitude of the pressure anomalies at the monitoring points in the overlying formation.

Residual Analysis

Residual analysis provides a measure of the overall goodness-of-fit. Figure 9 presents, the residuals ($r = z^* - z$) of the disparity between the measured pressures (z^*) and

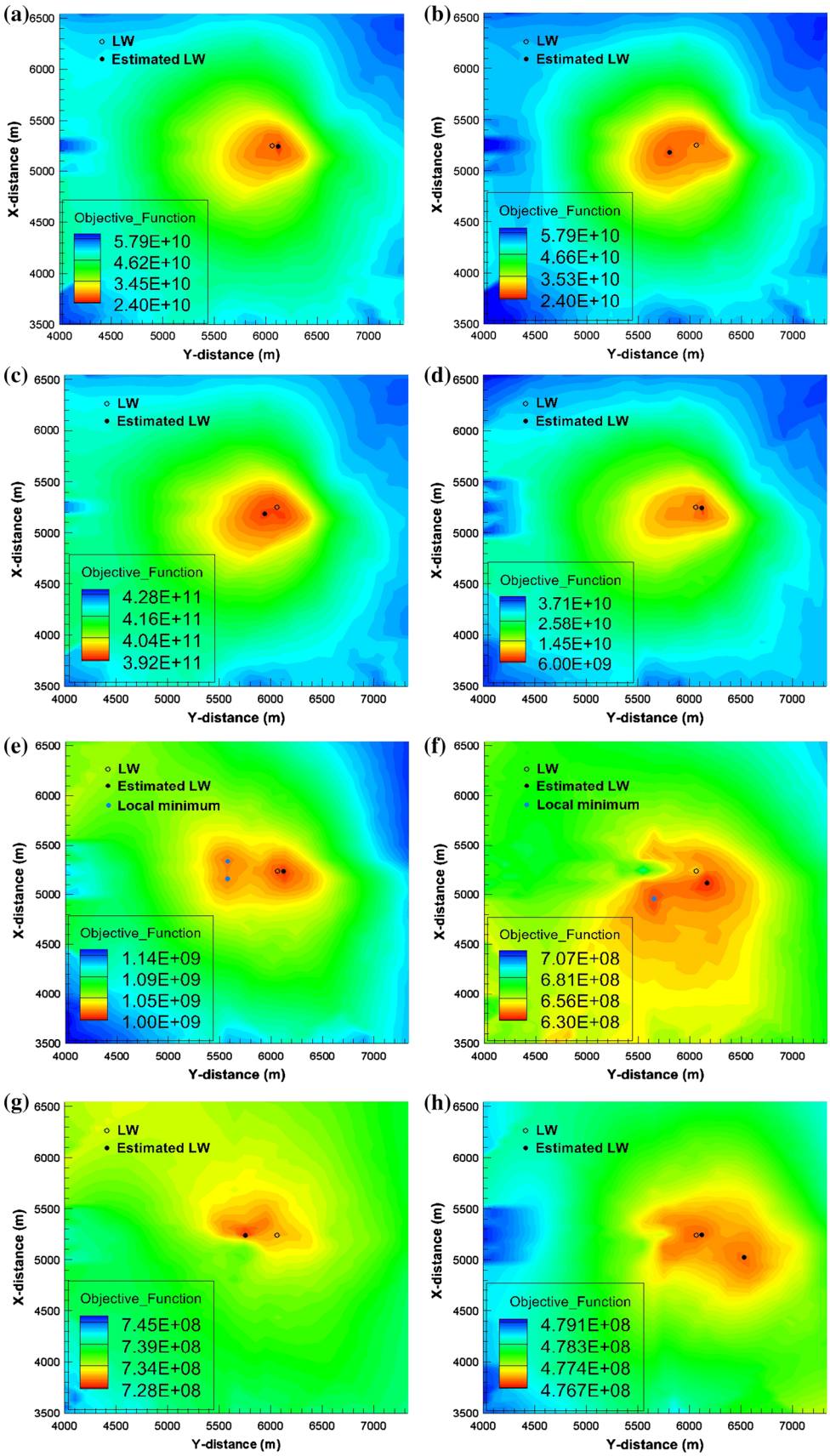

Fig. 8 Estimated leakage pathway location from objective function in **a** case 1, **b** case 2, **c** case 3, **d** case 4, **e** case 5, **f** case 6, **g** case 7, and **h** case 8

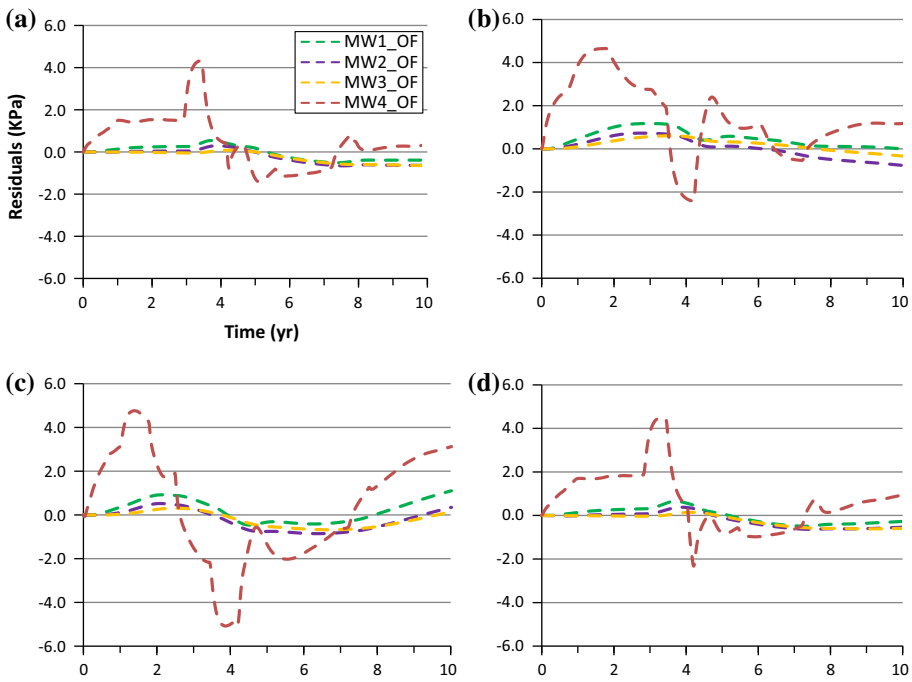

Fig. 9 Residuals in the overlying formation in each simulation case for **a** case 1, **b** case 2, **c** case 3, and **d** case 4

calculated pressures (z) in the overlying formation for cases 1 through 4. The residuals of the storage formation in the same scenarios are shown in Fig. 10. In Fig. 9, the residuals for case 2 (Fig. 9b) and case 3 (Fig. 9c) are larger than those for case 1 (Fig. 9a) and case 4 (Fig. 9d), indicating that the inversions of cases 2 and 3 have lower accuracy. On the other hand, in Fig. 10, the residuals for the storage formation in each case are not identical to the different estimated results from each case, although the residuals in case 3 (Fig. 10c) are larger than those in case 4 (Fig. 10d). This result implies that the pressure data in the storage formation may not be suitable for estimating leakage pathway locations because the sensitivity of the monitoring wells in the storage formation is very slight to changes in leakage pathway permeability, i.e., leakage rates (see Fig. 7). The large amount of injected CO_2 can damp the pressure anomalies induced by leaks in the storage formation. However, pressure anomalies in the overlying formation that are induced by leaks can be critical for detecting likely leakage pathway locations by inverse modeling. To demonstrate these results, two inverse models were conducted based on the "idealized case". First, the inverse analysis estimated the leakage pathway location based on only measurement data in the overlying formation (Fig. 11a). The second inversion estimated the leakage location based only on the measurement data in the storage formation (Fig. 11b). In Fig. 11a, the leakage pathway was estimated similarly to case 1 but the second inversion was ill-posed. These inverse modeling results identify that pressure anomalies induced by leaks in the overlying formation are critical for detecting the leakage pathway locations. Thus, calculating the exact pressure anomalies in the overlying formation is very important for successful leakage pathway estimation. The significant influential factors on calculating the pressures in the overlying formation should be parameterized to reduce those impacts on the leakage pathway detection.

Another interesting observation is that even the idealized case has some residuals in all of the four monitoring wells in Fig. 9a. In particular, the residuals in MW4, including serious pressure anomalies associated with capillary effects at the leakage pathway, are relatively very large. The residuals are caused by increased truncation errors, derived from the adjustments in the number of grid blocks in the model domain to reduce the computational demands for inverse modeling. Thus, the drifts in time from the increased truncation errors when CO_2 reaches the bottom of the leakage pathway result in the significant residuals at MW4. Such truncation errors can cause these deviations (between the actual and estimated leakage pathway locations) in the inverse modeling results. In the model domain, the intervals of the initial guesses for the leakage pathway are at most 100 m. To alleviate the deviations of the inverse modeling results, a model with finer intervals for the initial guesses is required.

The storage formation in which CO_2 is injected has higher pressure than the overlying formation, so the residuals in the storage formation can be larger. Such contrast may lead to a failure of the inverse model solution because the residuals in the overlying formation, which are critical for leakage pathway detection, can be obscured. In Figs. 9 and 10, the magnitude of the residuals in the storage

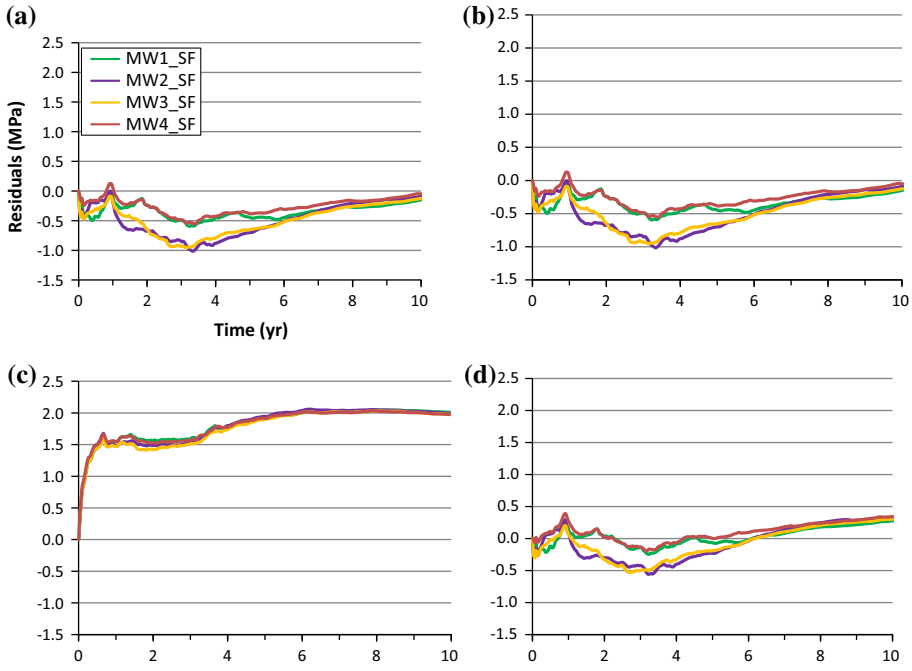

Fig. 10 Residuals between measured and calculated pressures in the storage formation in each simulation case for **a** case 1, **b** case 2, **c** case 3, and **d** case 4

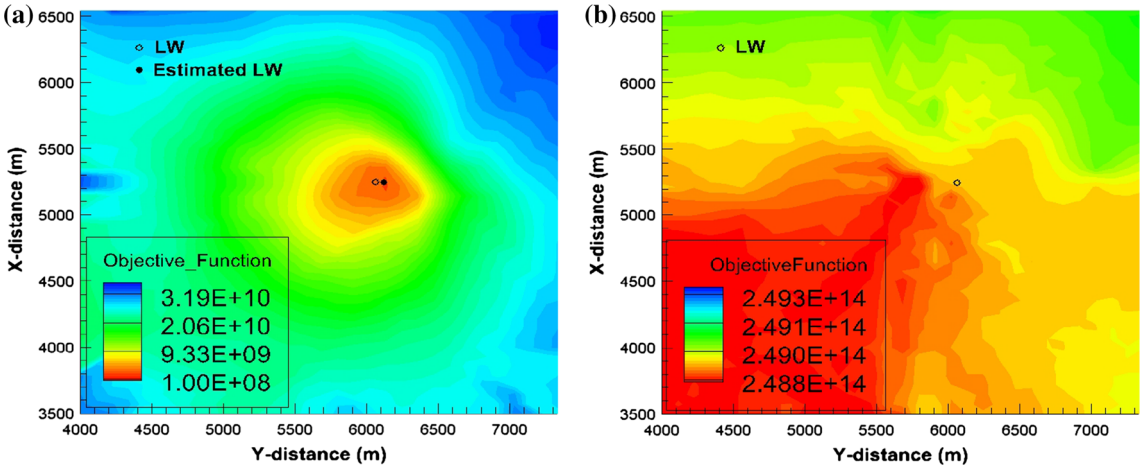

Fig. 11 Estimated leakage pathway location from the objective function **a** using measurements in the overlying formation and **b** using measurements in the storage formation

formation is approximately 100 times larger than that in the overlying formation. Therefore, in cases 1 through 8, 1 Pa and 100 Pa weighting factors were utilized for the overlying and storage formations, respectively, so that the residuals of both formations will be approximately equivalent.

Effect of singular noises in the measurements

Figure 12 illustrates, each inversion result of cases 9 through 13 correspondingly applied to cases 4 through 8 with the measured signals, including random noises. Case 9 determined that the most probable leakage pathway is located at $(x, y) = (5250, 6150$ m) as shown in Fig. 12a. The deviation from the actual leakage pathway is 100 m, indicating that the leakage pathway was reasonably estimated, as in case 4 (see Fig. 8d). The result of case 10 (see Fig. 12b) also has an analogy with that of case 5 (see Fig. 8e), i.e., though this inversion estimated one global minimum and one local minimum, the global minimum is not significantly different from the actual leakage pathway. However, as shown in Fig. 12c–e, the accuracies of each estimated leakage location in cases 11, 12, and 13 decrease more than those in cases 6, 7, and 8 (see Fig. 8f–h) because of the effect of noises in the measurements. In particular, the inverse modeling of case 13 was ill-posed. A noise problem in the measurements can be significant for leakage pathway detection by inverse modeling and degrade the

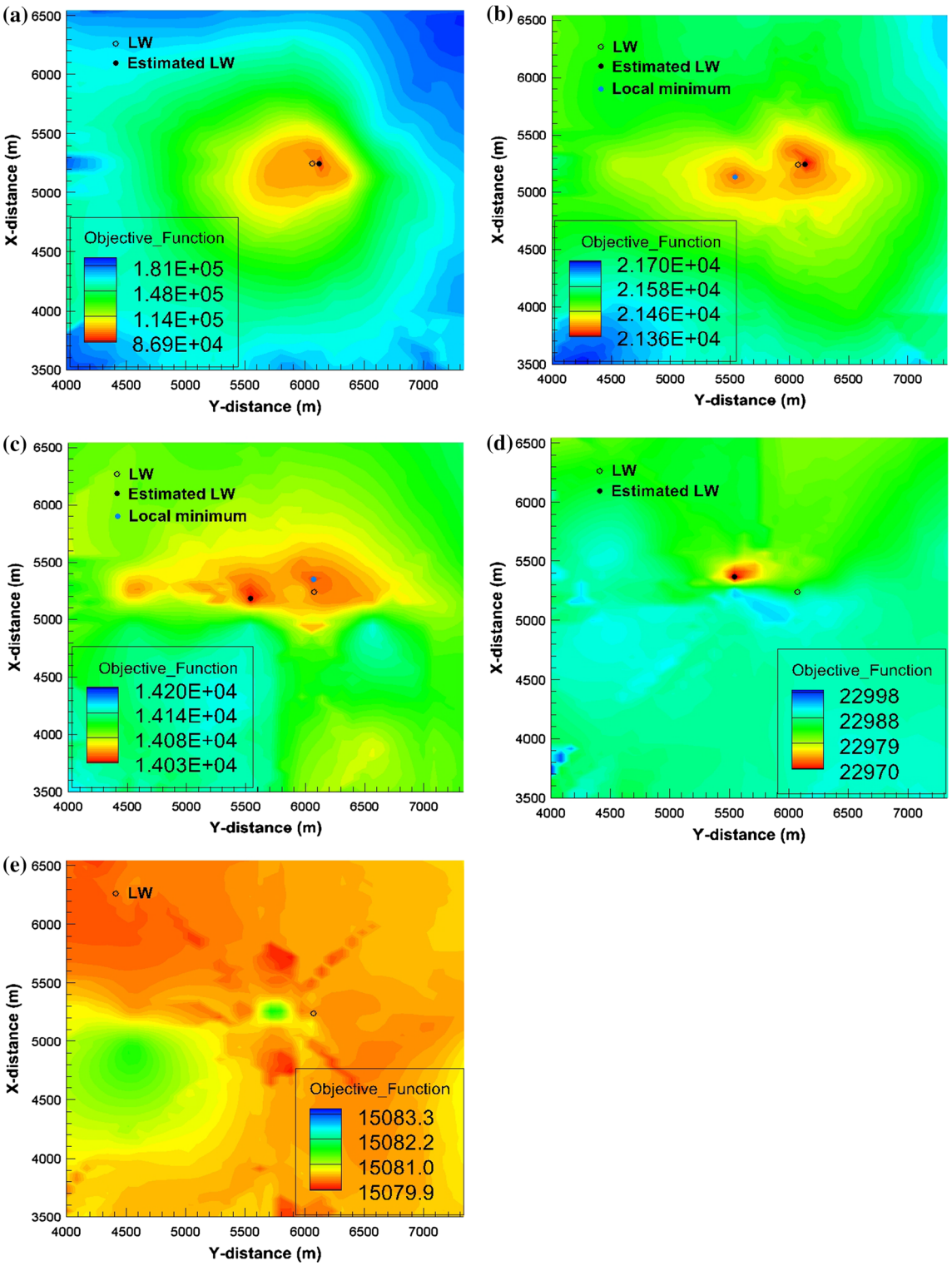

Fig. 12 Estimated leakage pathway location from the objective function in **a** case 9, **b** case 10, **c** case 11, **d** case 12, and **e** case 13 using measurements with random noises

accuracy of the leakage pathway estimation depending on the number of monitoring wells and the monitoring periods associated with the magnitude of the measured pressure anomalies induced by leaks (see "Appendix 2" section). Table 7 presents the objective function values and coordinates of the estimated leakage locations in thirteen cases. In Table 7, the inversions from measurement data noises (cases 9 through 13) have much smaller objective function

Table 7 Objective function values and coordinates of the estimated leakage locations in thirteen inversion scenarios (True: actual leakage pathway located at 23th initial guess)

Case	# of initial guess 23 (true)	Coordinate of estimated leakage location (m) (5250, 6050)	Deviation from true (m) –	Objective function –
1	24	(5250, 6150)	100	0.2554e11
2	10	(5150, 5750)	316	0.2657e11
3	11	(5150, 5950)	141	0.3936e12
4	24	(5250, 6150)	100	0.6697e10
5	24	(5250, 6150)	100	0.1009e10
6	13	(5150, 6150)	141	0.6387e9
7	21	(5250, 5750)	300	0.7304e9
8	24	(5250, 6150)	100	0.4768e9
	6	(4950,6550)	583	0.4768e9
9	24	(5250, 6150)	100	0.9092e5
10	24	(5250, 6150)	100	0.2138e5
11	9	(5150, 5550)	510	0.1403e5
12	31	(5350, 5550)	510	0.2297e5
13	Ill-posed	–	–	–

values than cases 1 through 8 because weighting factors of approximately 600 and 80,000 Pa were assigned for the overlying and storage formations, respectively; i.e., those weighting factors are approximately assessed based on the standard deviation of the random data errors and the different magnitudes of the residuals of the overlying and storage formations.

In this study, the random data errors including noises of 0.1 % were applied to leakage pathway estimation. However, measurements including the various magnitudes of random noises need to be applied to quantitatively identify the impacts of measurement data noises on the application of inverse modeling, and more studies should be conducted with respect to the complexities of uncertain input parameters and model geometry.

Conclusion

The conceptual domain was applied to model the effects of CO_2 and brine migrations through the leakage pathway. In the modeling scenario, CO_2 is injected for 10 years into the storage formation. The increased pressure gradient from the CO_2 injection continuously induces brine discharges through the leakage pathway before the CO_2 leaks. When CO_2 reaches the bottom of the leakage pathway after approximately 3.5 years, CO_2 migration along a leakage pathway saturated by brine induces capillary effects. Each pressure profile at the four monitoring wells (MW1, MW2, MW3, and MW4) in the overlying reservoir has a sudden change in the pressure due to the capillary effects at the leakage pathway. This process has a substantial effect on MW4 in the overlying formation, which is the closest monitoring well to the leakage pathway.

The sensitivity analysis was performed through the sigma-normalized coefficient with respect to four parameters: the vertical permeability of the leakage pathway (k_{lz}), permeability of the overlying formation k_O, permeability of the storage formation k_S, and caprock permeability (k_C). As a result, the most influential input parameters on the pressure signals at the MWs are both k_O and k_S. The sensitivity of k_{lz} for the MWs in the overlying formation are significantly larger than that in the storage formation.

In the inverse modeling, the leakage pathway location was estimated by calibrating the logarithm of the absolute vertical permeability for each different initial guess location of the leakage pathway. Depending on the results of the sensitivity analysis, the uncertainties of the reservoir permeability values in the inverse modeling were employed and the uncertain reservoir permeability values were parameterized to reduce those impacts on the leakage pathway estimation. In thirteen inverse modeling scenarios, the accuracy of the leakage pathway detection can significantly depend on the number of monitoring wells and the magnitude of the pressure anomalies. In addition, the noises in the measurements reduce the accuracy of the leakage pathway detection. Case 5 and case 10, each using pure and noisy monitoring data from MW1, MW2, and MW3 over 3 years, sustained an accuracy of the leakage pathway estimation similar to that of the idealized case. Residual analysis illustrated that critical information for leakage pathway estimation by the inverse modeling is the pressure anomalies in the overlying formation induced by

leaks. This indicates that prior information about the input parameters that are influential for calculating pressures in the overlying formation is very important for successful leakage pathway detection. In addition, the influential factors should be parameterized to reduce the impact on the leakage pathway estimation.

In a follow-up study, multiple leakage pathways should be pursued to evaluate the applicability of the inverse method. Pressure signals from multiple leakage pathways can be distributed, creating further complexity. The uncertainties of multiple input parameters and model geometry can also have a more significant impact on the detection of leakage pathways. Uncertain pore compressibility can have an effect on the pressure's evolution in a confined aquifer, so the compressibility may be considered as one of the influential uncertain parameters. The drift in pressure gauges can limit the applicability of inverse modeling. Those will be quantitatively examined in a future study. An uncertain leakage pathway size may create errors in the calculation of pressure anomalies induced by leaks. The parameterization of the leakage pathway geometry will be studied for a more effective inversion. Most of all, an inversion in an unknown heterogeneity will be a difficult problem and challenge. The inverse modeling may be incorporated with geostatistics to estimate the heterogeneity and leakage pathways. The above follow-up study will proceed to provide practical strategies for leakage detection and subsurface monitoring in a GCS project.

Acknowledgments This study was supported by the Department of Energy (DOE), a United States government agency, under contract number DE-FC26-05NT42591.

Appendix 1

The effect of caprock thickness on the pressure anomalies could be examined from the pressure difference dP, calculated from pressures in the overlying formation between (1) with the leakage pathway and (2) without the leakage pathway in the model domain of Fig. 1. The thickness of the caprock is varied to 60, 80, 100, and 120 m, but the other simulation conditions are the same as those of the model domain. Figure 13 depicts, the dP in the overlying formation for each caprock thickness after 10 years.

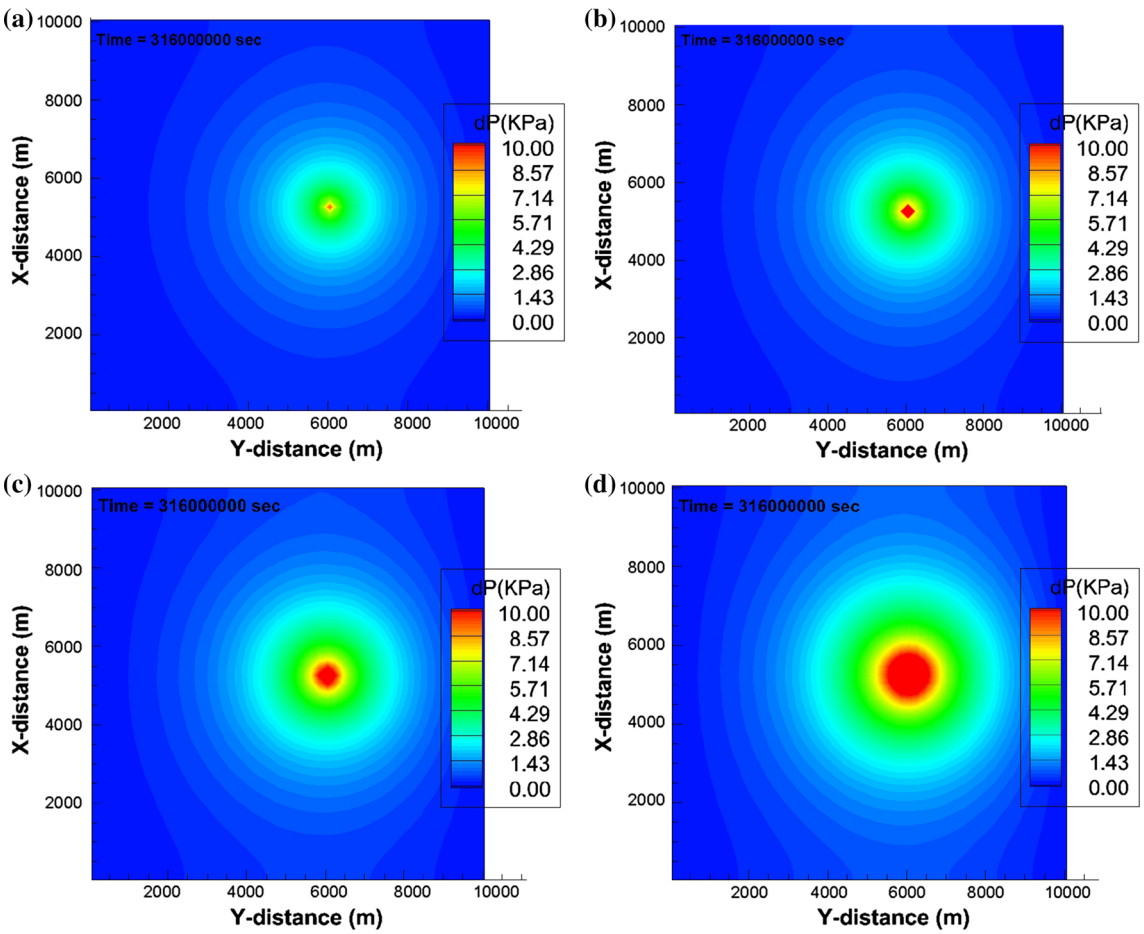

Fig. 13 Pressure differential results with caprock thickness: **a** 60 m, **b** 80 m, **c** 100 m, and **d** 120 m after 10 years

In Fig. 13, the d*P* and the area significantly decrease as the thickness of the seal layer decreases. The reason is that CO_2 or brine may diffuse through thinned caprock (without leakage pathways) more quickly, so d*P* may be reduced for cases of greater diffusion through the caprock. The diffusion process, therefore, may reduce the efficacy of leakage pathway detection by inverse analysis. That is, thicker caprock can reduce diffusion and thus magnify pressure anomalies related to leakage pathways for successful inverse modeling. This effect can be a criterion for the siting and screening of CO_2 injection projects designed to better identify leaks using inverse modeling.

Appendix 2

The magnitude of pressure anomalies induced by leakage with respect to the monitoring wells increases as the monitoring periods increase in a system with constant CO_2 injection. The pressure anomalies from leaks were examined by pressure difference (d*P*) as mentioned in "Appendix 1" section. Figure 14 presents, the d*P* at four monitoring wells in the overlying formation for 10 years of simulated time. In Fig. 14, each d*P* value at MW1, MW2, and MW3 is approximately 0.58, 0.32 and 0.12 kPa for a 1-year monitoring time and 1.84, 1.36 and 0.84 kPa for 3 years. The results of both case 5 under a no-noise condition (Fig. 8e) and case 10 under noisy conditions (Fig. 12b) for monitored data from MW1, MW2, and MW3 over 3 years sustained good accuracy for the leakage pathway estimation, although the combination of those d*P* dimensions cannot be defined as a limit for the leakage pathway detection. The accuracy (or limit) of leakage detection using inverse analysis can significantly depend on the number of monitoring wells, the magnitude of the pressure anomalies, the relative distance between the monitoring wells and leakage pathways and the monitoring period.

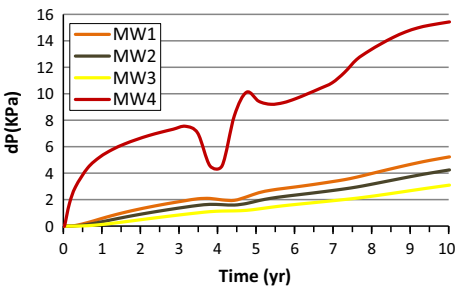

Fig. 14 Pressure differential results at four monitoring points in the overlying formation for 10 years of simulated time

References

Altevogt AS, Celia MA (2004) Numerical modeling of carbon dioxide in unsaturated soils due to deep subsurface leakage. Water Resour Res 40:W03509. doi:10.1029/2003WR002848

Carroll S, Hao Y, Aines R (2009) Transport and detection of carbon dioxide in dilute aquifers. Energy Procedia 1:2111–2118

Cihan A, Zhou Q, Birkholzer JT (2011) Analytical solutions for pressure perturbation and fluid leakage through aquitards and wells in multilayered-aquifer systems. Water Resour Res 47:W10504. doi:10.1029/2011WR010721

Cihan A, Birkholzer JT, Zhou Q (2013) Pressure buildup and brine migration during CO_2 storage in multilayered aquifers. Groundwater 51:252–267

Corey AT (1954) The interrelation between gas and oil relative permeabilities. Prod Mon 19:38–41

Doughty C, Pruess K (2004) Modeling supercritical carbon dioxide injection in heterogeneous porous media. Vadose Zone J 3:837–847

Finsterle S (2007) iTOUGH2 user's guide. Lawrence Berkeley National Laboratory, Berkeley, CA

Gasda SE, Bachu S, Celia MA (2004) Spatial characterization of the location of potentially leaky wells penetrating a deep saline aquifer in a mature sedimentary basin. Environ Geol 46:707–720

Gasda SE, Wang JZ, Celia MA (2011) Analysis of in situ wellbore integrity data for existing wells with long-term exposure to CO_2. Energy Procedia 4:5406–5413

Hou Z, Murray JC, Rockhold LM (2012) CO_2 migration in intact caprock and leakage risk in three-dimensional heterogeneous formations. Paper presented at the The Eleventh Annual Carbon Capture, Utilization & Sequestration Conference, Pittssburgh, PA, April 30 2012

Jung Y, Zhou Q, Birkholzer JT (2012a) Early detection of brine or CO_2 leakage through high-permeability pathways using pressure-based monitoring data. Paper presented at the The Eleventh Annual Carbon Capture, Utilization & Sequestration Conference, Pittsburgh, PA, April 30 2012

Jung Y, Zhou Q, Birkholzer JT (2012b) Impact of data uncertainty on identifying leakage pathways in CO_2 geologic storage systems and estimating their hydrogeological properties by inverse modeling. Paper presented at the TOUGH Symposium, Lawrence Berkeley National Laboratory, Berkeley, CA, September 17 2012

Jung Y, Zhou Q, Birkholzer JT (2013) Early detection of brine and CO_2 leakage through abandoned wells using pressure and surface-deformation monitoring data: Concept and demonstration. Adv Water Resour 62:555–569

Krevor S, Perrin J-C, Esposito A, Rella C, Benson S (2010) Rapid detection and characterization of surface CO_2 leakage through the real-time measurement of δ13 C signatures in CO_2 flux from the ground. Int J Greenhouse Gas Control 4:811–815

Metz B, Davidson O, de Coninck H, Loos M, Meyer L (2005) IPCC special report on carbon dioxide capture and storage. Cambridge University Press, New York, NY

Mualem Y (1976) A new model for predicting the hydraulic conductivity of unsaturated porous media. Water Resour Res 12:513–522

Nogues JP, Nordbotten JM, Celia MA (2011) Detecting leakage of brine or CO_2 through abandoned wells in a geological sequestration operation using pressure monitoring wells. Energy Procedia 4:3620–3627

Nordbotten JM, Celia MA, Bachu S (2004) Analytical solutions for leakage rates through abandoned wells. Water Resour Res 40:W04204. doi:10.1029/2003WR002997

Nordbotten JM, Kavetski D, Celia MA, Bachu S (2008) Model for CO_2 leakage including multiple geological layers and multiple leaky wells. Environ Sci Technol 43:743–749

Onuma T, Ohkawa S (2009) Detection of surface deformation related with CO_2 injection by DInSAR at In Salah, Algeria. Energy Procedia 1:2177–2184

Pruess K (2005) ECO2N: a TOUGH2 fluid property module for mixtures of water, NaCl, and CO_2. Lawrence Berkeley National Laboratory, Berkeley, CA

Pruess K, García J (2002) Multiphase flow dynamics during CO_2 disposal into saline aquifers. Environ Geol 42:282–295

Pruess K, Moridis G, Oldenburg C (1999) TOUGH2 user's guide, version 2.0. Lawrence Berkeley National Laboratory, Berkeley, CA

Saltelli A, Chan K, Scott EM (2000) Sensitivity analysis, vol 134. Wiley, New York

van Genuchten MT (1980) A closed-form equation for predicting the hydraulic conductivity of unsaturated soils. Soil Sci Soc Am J 44:892–898

Zhou Q, Birkholzer JT, Tsang C-F (2009) A semi-analytical solution for large-scale injection-induced pressure perturbation and leakage in a laterally bounded aquifer–aquitard system. Transp Porous Media 78:127–148